RSC Advances

ROYAL SOCIETY OF CHEMISTRY

www.rsc.org/advances

Cite this: DOI: 10.1039/c0xx00000x

www.rsc.org/xxxxxx

ARTICLE TYPE

Construction of Fe6, Fe8 and Mn8 Metallamacrocyclic Complexes and Magnetic Properties

Huijun Li,[a] Yuan Wang,[a] Hongxin Cai,[a] Zhouqing Xu *[a], Lei Jia*[a] and Hongwei Hou*[b]

Received (in XXX, XXX) Xth XXXXXXXXX 20XX, Accepted Xth XXXXXXXXX 20XX
First published on the web Xth XXXXXXXXX 20XX
DOI: 10.1039/b000000x

By treating $FeSO_4$ or $Mn(OAc)_2$ with 5'-(pyridin-2-yl)-2H,4'H-3,3'-bi(1,2,4-triazole) (H_2pbt), three novel metallamacrocycle-based complexes $[Fe(Hpbt)(C_2O_4)_{0.5}]_n$ (**1**), $\{[Fe(pbt)(H_2O)]\cdot 2H_2O\}_n$ (**2**), $\{[Mn(pbt)(H_2O)]\cdot 2EtOH\cdot 0.5H_2O\}n$ (**3**) have been synthesized and characterized. In **1**, the hexanuclear metallamacrocycle units are connected with each other resulting in the formation of two-dimensional frameworks. Octanuclear metallamacrocycle-based complexes **2** and **3** display three-dimensional porous frameworks. Interestingly, left- and right-handed helical chains present alternately along the crystallographic *c* axis in **2** and **3**. Magnetic susceptibility measurements show that the three complexes display different antiferromagnetic coupling intensities.

Introduction

Polynuclear metallamacrocycles exhibit excellent feasibility in diverse applications, such as heterogeneous catalysis, magnetic materials, gas storage and separation, mainly due to the fact that these complexes combine novel structural features and excellent metallamacrocycle properties.[1-5] Especially, polynuclear metallamacrocycles containing of paramagnetic 3d metal ions have attracted intense interests because their specific structure geometries and various coordination modes make them a good platform for exploring magneto-structural correlations resulting from the mutual interactions among metal centers.[6-8] When acting as structural and/or functional building units, they can endow such complexes combining novel structural features with retention and possible enhancement of the magnetic properties of adjacent centers.[9] Up to now, several magnetic metallamacrocycle complexes have been reported.[10-13] The formation of these complexes, although seemingly serendipitous, reveals a prevalent feature that the metal ions are connected by the chelation of adjacent pyrazol, triazole, and/or pyridine groups of a rigid multi-azacyclo organic ligands, which hints that such complexes can be assembled into coordination polymers if the organic ligands are polytopic.[14-15]

Taking above factors into account, the crucial factor for constructing polynuclear metallamacrocycle is to select organic linkers with suitable shape, functionality and symmetry. It is well known that triazole ring possesses aromaticity and multiple coordinating modes, which can offer multiple coordinating sites for bridging closely, situated metal ions, sustaining a diversity of polynuclear and even macrocyclic motifs.[16] 3,5-position substituted 1,2,4-triazole derivatives should be a kind of appropriate ligand favouring the occurrence of polynuclear macrocycle by the fact that they unite the coordination geometries of pyrazoles, imidazoles and additional donor groups substituted at the 3,5-position, and exhibit excellent properties of acting as bridging ligands.[17-18] These properties make them show strong capacity to connect metal ions to a metallamacrocycle and shorten the distance between metal ions, which could create an effective magnetic exchange pathway and provide a platform to investigate the magneto-structural correlations.[19-23] In this article, 5'-(pyridin-2-yl)-2H,4'H-3,3'-bi(1,2,4-triazole) (H_2pbt), a chelating bridging 1,2,4-triazole derivative, was used to construct three novel metallamacrocycle-based complexes $[Fe(Hpbt)(C_2O_4)_{0.5}]_n$ (**1**), $\{[Fe(pbt)(H_2O)]\cdot 2H_2O\}_n$ (**2**),

a The Department of Physics and Chemistry, Henan Polytechnic University Jiaozuo, 454000, P. R. China. E-mail: zhqxu@hpu.edu.cn. Tell: (+86) 391–3987811.

b The Colloge of Chemistry and Molecular Engineering, Zhengzhou University, Zhengzhou, Henan, 450052, P. R. China. E-mail: houhongw@zzu.edu.cn. Fax: (86) 0371-67761744;

*†Electronic supplementary information (ESI) available: selected bond lengths and bond angles, additional figures, powder X-ray patterns, TGA curves for complexes **1**–**3**. CCDC reference numbers: 1408068, 1408069 and 908080 for **1**–**3**. For ESI and crystallographic data in CIF or other electronic format see DOI:10.1039/b000000x/*

$\{[Mn(pbt)(H_2O)]\cdot 2EtOH\cdot 0.5H_2O\}_n$ (**3**) based on Fe6, Fe8 and Mn8 metallamacrocycle units, respectively. Magnetic susceptibility measurements show that the three complexes display different antiferromagnetic coupling intensities.

Experimental section

Materials and Physical Measurements. All chemical reagents were purchased from Jinan Henghua Sci. & Tec. Co. Ltd. without further purification. IR data were recorded on a BRUKER TENSOR 27 spectrophotometer with KBr pellets in the region of 400 – 4000 cm^{-1}. Elemental analyses (C, H and N) were carried out on a Flash EA 1112 elemental analyzer. Powder X-ray diffraction (PXRD) patterns were recorded using CuKα radiation on a PANalytical X'Pert PRO diffractometer. Thermal analyses were performed on a Netzsch STA 449C thermal analyzer at a heating rate of 10 °C min^{-1} in air.

Synthesis

Synthesis of $[Fe(Hpbt)(C_2O_4)_{0.5}]_n$ (1): A mixture of $FeSO_4\cdot 7H_2O$ (27.8 mg, 0.1 mmol), H_2pbt (10.6 mg, 0.05 mmol), KSCN (9.7 mg, 0.1 mmol), oxalic acid (12.6 mg, 0.1 mmol), H_2O and CH_3CH_2OH (5+5mL) were sealed in a Teflon-lined stainless steel container and heated at 160°C for 4 days. After slowly cooling to room temperature at a rate of 5 °C/h, orange prismatic crystals of **1** were acquired in 57% yield. Elemental analysis data calcd for $C_{10}H_6FeN_7O_2$: C 38.49 H 1.94 N 31.42%. Found: C 38.27, H 1.77, N 31.51%. IR: 3446 (s), 2955 (s), 1642 (m), 1618 (m), 1550 (w), 1468 (m), 1436 (m), 1368 (m), 1322 (m), 1121 (m), 1048 (w), 799 (w), 752 (w), 718 (w), 645 (w), 596 (w).

Synthesis of $\{[Fe(pbt)(H_2O)]\cdot 2H_2O\}_n$ (2): A mixture of $FeSO_4\cdot 7H_2O$ (27.8 mg, 0.1 mmol), H_2pbt (10.6 mg, 0.05 mmol), KSCN (9.7 mg, 0.1 mmol), H_2O and DMF (5+5mL) was sealed in a Teflon-lined stainless steel container and heated at 160°C for 4 days. After slowly cooling to room temperature at a rate of 5 °C/h, orange prismatic crystals of **2** were acquired in 62% yield. Elemental analysis data calcd for $C_9H_{12}FeN_7O_3$: C 33.56 H 3.76 N 30.44%. Found: C 33.47, H 3.59, N 30.69%. IR: 3447 (s), 1641 (s), 1619 (s), 1553 (s), 1467 (s), 1439 (m), 1318 (m), 1120 (m), 1050 (w), (m) 802 (w), 755 (w), 722 (w), 648 (w), 594 (w).

Synthesis of $\{[Mn(pbt)(H_2O)]\cdot 2EtOH\cdot 0.5H_2O\}_n$ (3): A mixture of $Mn(OAc)_2\cdot 4H_2O$ (10.7 mg, 0.05 mmol), H_2pbt (10.6 mg, 0.05 mmol), H_2O and CH_3CH_2OH (5+5mL) was sealed in a Teflon-lined stainless steel container and heated at 80°C for 3 days. After slowly cooling to room temperature, colorless crystals of **3** were acquired in 32% yield. Elemental analysis data calcd for $C_{26}H_{40}N_{14}Mn_2O_7$: C 40.52, H 5.23, N 25.44%. Found: C 40.45, H 5.34, N 25.58%. IR: 3446 (s), 1636 (s), 1605 (s), 1428 (s), 1329 (s), 1132 (s), 1146 (m), 1108 (m), 1017 (m), 997 (w), 794 (w), 723 (w), 672 (w).

Crystal Data Collection and Refinement. Crystals of **1-3** were performed using Rigaku CrystalClear-SM Expert 2.0 diffractometer equipped with graphite monochromatic Mo-Kα radiation (λ = 0.71073 Å). The structures were solved by the direct method and refined by the full-matrix least-squares method on F with anisotropic thermal parameters for all non-hydrogen atoms.[24] Hydrogen atoms were located geometrically and refined isotropically.

Results and discussion

The Description of Crystal Structures. Single crystal X-ray crystallographic analysis reveals that complex **1** displays a 3D network and crystallizes in a *monoclinic* system, space group *P21/n*. As shown in Figure 1a, the asymmetry structure of **1** includes one Fe^{2+} ion, one pbt^{2-} and a half oxalate. The coordination environment of Fe^{2+} is six-coordinated (FeN_4O_2) with four nitrogen donors from two different $Hpbt^-$ and two oxygen atoms from one oxalate and adopts slightly distorted octahedron geometry. Each $Hpbt^-$ acts as bridging ligand coordinating with two Fe^{2+} ions through two chelate linkages. Four such ligands and two oxalate connect six Fe^{2+} forming an approximately coplanar hexanuclear metallamacrocycle unit (Figure 1b). The distances of adjacent Fe^{2+} ions are 6.22 and 5.57 Å, respectively. The hexanuclear units are connected with each other through the $Hpbt^-$ and oxalate resulting in the formation of two-dimensional layer (Figure 1c). The grid motif (39-membered metallocyclic rings) has the dimension of 11.84 × 14.89 Å (diagonal distances). In addition, the adjacent 2D layers in an offset way are arranged into three-dimensional supermolecular framework by strong hydrogen-bonding interactions and π···π interactions (Figure S2a and 2b). The π···π interaction exists between the nearest trizole ring and pyridine ring with the centroid-to-centroid separation of 3.885 Å. And the hydrogen-bonding interaction appears between adjacent ligands with D-H..A distance of 2.91 Å.

Table 1. Crystal data and structure refinement for complex **1-3**[a]

compound	1	2	3
Formula	$C_{10}H_6FeN_7O_2$	$C_9H_{12}FeN_7O_3$	$C_{26}H_{40}Mn_2N_{14}O_7$
fw	312.07	321.10	772.62
T/K	293(2)	293(2)	296(2)
λ (Mo Kα), Å	0.71073	0.71073	0.71073
cryst syst	*Monoclinic*	*Tetragonal*	*Tetragonal*
space group	*p21/n*	*I41/a*	*I41/a*
a/Å	9.5236(19)	19.623(3)	19.692(9)
b/Å	12.240(2)	19.623(3)	19.692(9)
c/Å	9.907(2)	19.147(4)	20.101(20)
α/deg	90	90	90
β/deg	101.88(3)	90	90
γ/deg	90	90	90
V/Å^3	1130.2(4)	7373(2)	7795(9)
Z	4	16	8
$D_{calcd.}$(g·cm^{-3})	1.834	1.157	1.317
F(000)	628	2624	3216
$2\theta_{max}$(°)	25.50	25.00	25.50
GOF	1.178	1.077	0.980
R_1(I>2sigma(I))	0.0416	0.0580	0.0608
wR_2 (all data)	0.0942	0.1534	0.1617

[a] $R_1 = ||F_o| - |F_c||/\square |F_o|$. [b] $wR_2 = [w(F_o^2 - F_c^2)^2/\square w(F_o^2)^2]^{1/2}$.

Although the molecular formulas of compound **2** and **3** are different, they are isostructural. Both of the two complexes have the same space group and unit-cell dimension. And the types and the positions of atoms in both are analogous. Therefore, only the structure of **2** will be discussed herein. Red crystal of **2** crystallizes in the tetragonal *I41/a* space group and displays a 3-connected three-dimensional framework. In the asymmetric unit of **2**, there is one crystallographically independent Fe^{2+} ion, one pbt^{2-} ligand, one coordinated water molecule and two lattice water molecules. Each Fe^{2+} ion is six-coordinated by five N

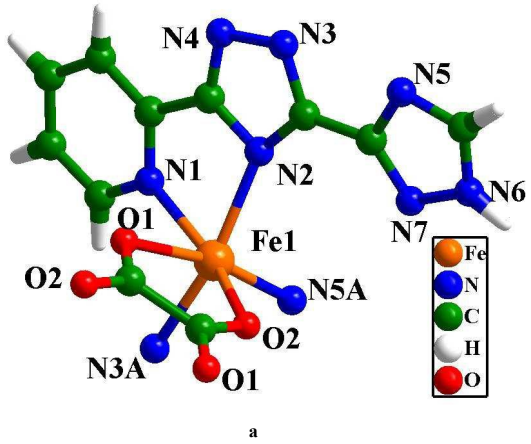

a

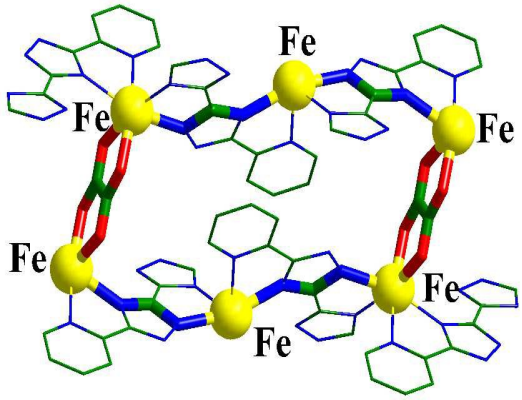

b

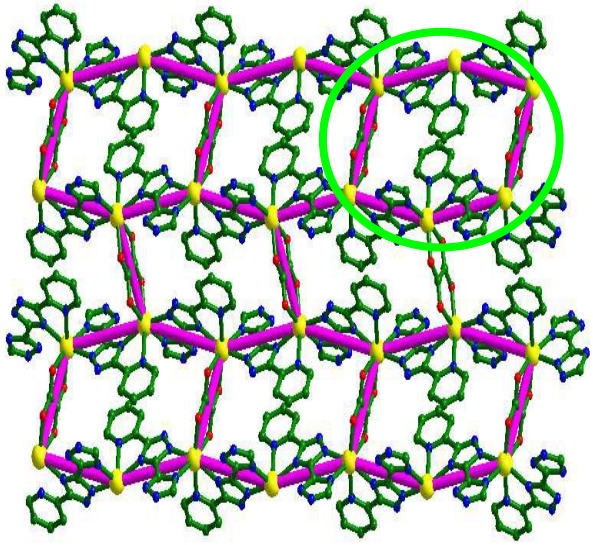

c

Figure 1. (a) The coordination environment of Fe^{2+} in polymer **1**. (b) The hexanuclear unit; (c) the two-dimensional network (Hydrogen atoms and water molecules are omitted for clarity in b and c).

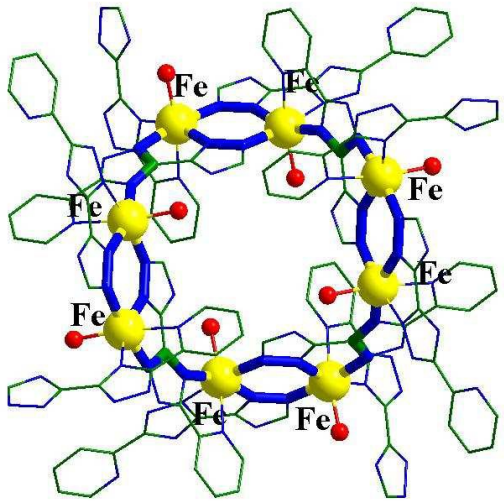

a

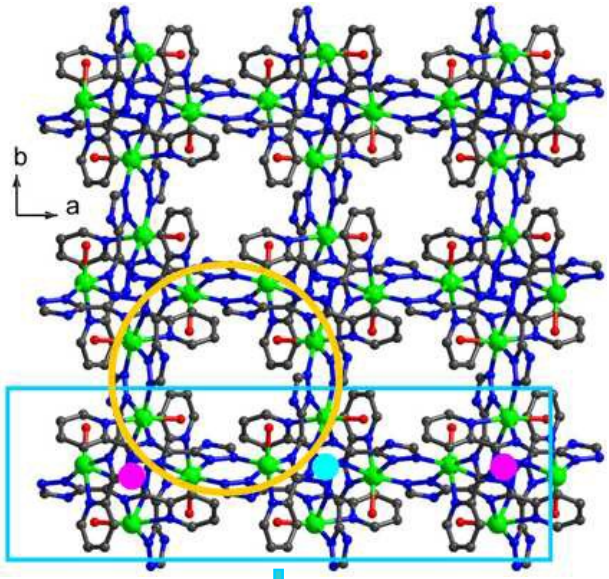

b

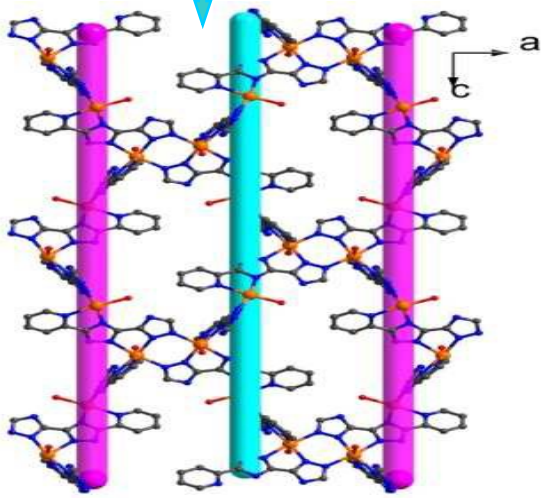

c

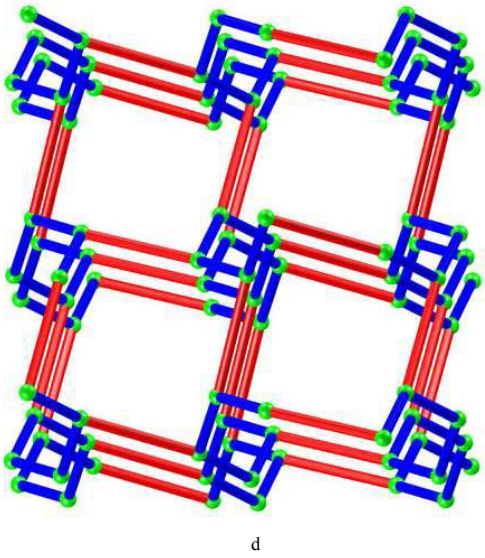

d

Figure 2. (a) the two-dimensional framework; (b) the octanuclear Fe unit; (c) the left- and right-helical chains; (d) the topology of the framework (Hydrogen atoms and water molecules are omitted for clarity).

atoms from three pbt^{2-} ligands, (two of them adopt bidentate chelating mode, while the remaining one uses a monedentate linkage), showing slightly distorted octahedral geometry (Figure S3). It is imperative to note here that eight Fe^{2+} ions are held together by the triazole groups of pbt^{2-} to form a butterfly-shaped octanuclear metallamacrocycle (Figure 2a). In the octanuclear metallamacrocycle unit, adjacent cations are linked by two ligands in different bridging modes: one is that the Fe-Fe vector is held by two bidentate N6, N7-bridged triazole group of pbt^{2-} ligand to form a dinuclear subunit, the other is that adjacent dinuclear units are linked by one N2, N4-bridged triazole group of pbt^{2-} ligand. The corresponding Fe-Fe distances are 4.23 and 6.31 Å, respectively. In addition, the pbt^{2-} ligands link the Fe^{2+} ions to generate left- and right-handed helical chains along the crystallographic *c* axis (Figure 2c). The resulting left- or right-handed helices with a pitch of 20.101 Å are alternately arranged in an equal ratio, generating an achiral layer parallel to the *bc* plane. Adjacent layers are connected through the Fe-N coordination bonds to form a 3D frameworks (Figure 2b). From the viewpoint of structural topology, each Fe^{2+} ion can be viewed as a 3-connected node. Thus, the whole framework of **2** can be topologically represented as a 3-connected *lig* net with the Schläfli symbol of (8^2. 10) (Figure 2d). The total solvent-accessible volume is approximately 49.5% calculated with PLATON software.

XRD Patterns and Thermal Analyses. To check the phase purity of the products, powder X-ray diffraction (PXRD) experiments have been carried out for these complexes (Figure S4). The peak positions of the experimental and simulated PXRD patterns are in good agreement with each other, indicating that the crystal structures are truly representative of the bulk crystal products. The differences in intensity may be owing to the preferred orientation of the crystal samples. The thermogravimetric analysis (TGA) (Figure S5) displays that

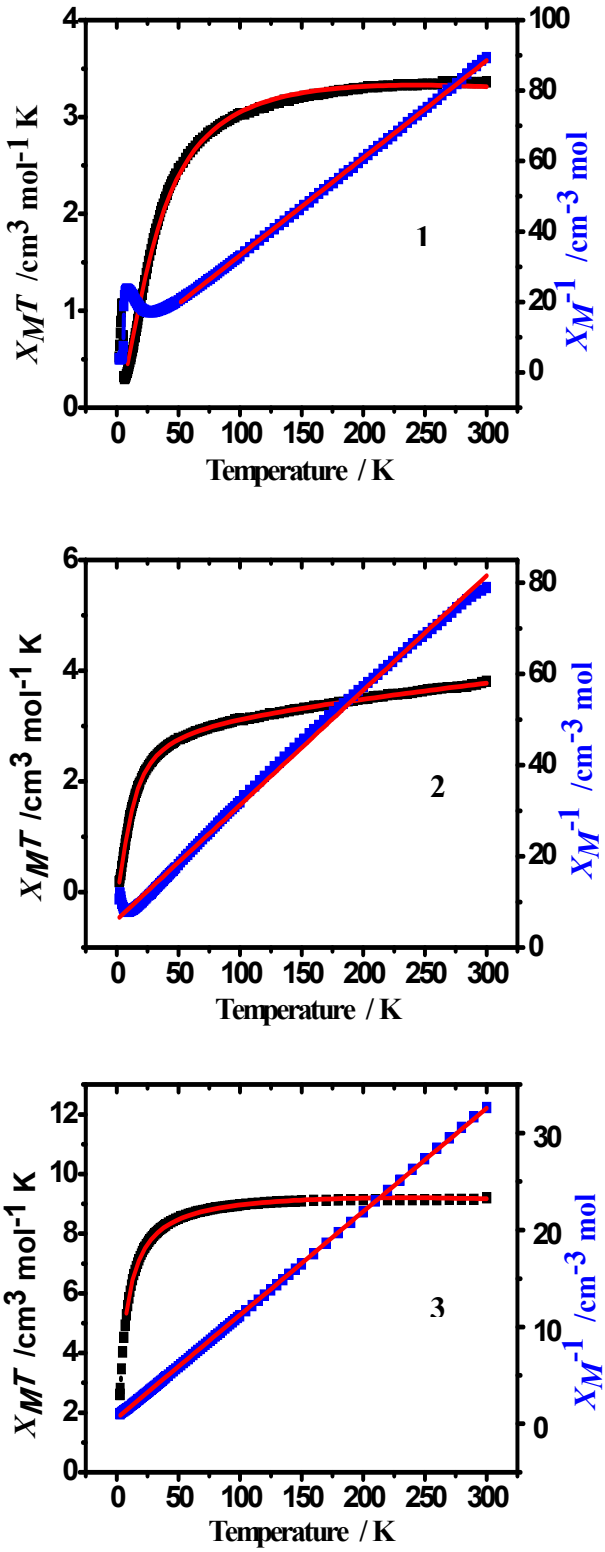

Figure 3. The $\chi_M T$ vs T plot and χ_M^{-1} vs T plot for polymers **1**-**3**.

complex **2** releases three water molecules in the range of 30−210 °C (found, 16.04%; calcd, 16.76%), complex **3** releases one and a half water molecules and two CH_3CH_2OH molecules in the range of 30−180 °C (found, 16.78%; calcd, 15.44%).

Maganetic Studies.

Variable-temperature magnetic susceptibility measurements of these complexes were carried out in the range of 2-300 K at 1000 Oe. As shown in figure 3a and 3b, the $\chi_M T$ values are 3.35 and 3.72 $cm^3 \cdot K \cdot mol^{-1}$ at 300 K for **1** and **2**, which are close to the expected value (3 $cm^3 \cdot K \cdot mol^{-1}$) of one magnetically isolated spin-only Fe^{2+} ion (S = 2, g = 2.0). When the temperature is decreased from 300 to 2 K, the $\chi_M T$ value continuously decreases and reaches the lowest measured temperature at 2 K. The χ_M^{-1} plots in the temperature range of 40-300K and 10-300K for **1** and **2** are linear, following the Curie-Weiss law with Weiss constants of θ = -23.42 and -20.7 K, Curie constants C = 3.84 and 3.71 $cm^3 \cdot K \cdot mol^{-1}$ for **1** and **2**, respectively. The negative value of θ and the total decrease of $\chi_M T$ should be attributed to the antiferromagnetic couplings between metal centers of the two complexes in the temperature range of 40-300K and 10-300K .

From the viewpoint of crystal structures of **1**, there are two bridges between adjacent Fe^{2+} ions, which are O-C-O and N-C-N bridges. But the magnetic interaction transmitted by N-C-N bridge could be ignored as the large distance between Fe^{2+} ions. For **2**, it could be presumed that the main magnetic interactions might happen between two triazole N6, N7-bridged Fe^{2+} ions, whereas the superexchange interactions through the triazole -N4-C7-N2- bridged Fe^{2+} ions can be ignored because of the long Fe···Fe distance. The magnetic susceptibility data were fitted assuming that the Fe^{2+} ions form an isolated spin dimer system. Therefore, a binuclear model is thus approximately analyzed by an isotropic dimer mode of spin S = 2. The spin Hamilton of this mode can be written as $\hat{H} = -2JS_1S_2$. The deduced expression of the molar susceptibility χ_m is: [25]

$$\chi_m = 2Ng^2\beta^2/KT((e^{2J/KT} + 5e^{6J/KT} + 14e^{12J/KT} + 30e^{20J/KT})/(1 + 3e^{2J/KT} + 5e^{6J/KT} + 7e^{12J/KT} + 9e^{20J/KT})) + TIP$$

where J is the exchange coupling parameter describing the magnetic interaction within the [Fe2] unit. The refinement converged at values of g = 2.03, J = -2.019 cm^{-1}, $TIP = 3\times10^{-5}$ emu, $R = 6.04\times10^{-4}$, and g = 2.09, J = -5.45 cm^{-1}, $TIP = -2\times10^{-5}$ emu, $R = 1.51\times10^{-4}$. The negative J values for **1** and **2** reveal the antiferromagnetic interactions between adjacent metal ions.

The temperature dependent magnetic property of **3** is illustrated in Figure 3c in the form of $\chi_M T$ and χ_M^{-1} versus T. The $\chi_M T$ value is 9.13 cm^3 K mol^{-1} at 300 K. On cooling, $\chi_M T$ falls to 2.6 cm^3 K mol^{-1} at 1.8 K. This magnetic behavior shows the typical characteristics of antiferromagnetism. The inverse magnetic susceptibility data in the temperature range 1.8 – 300 K were fitted with the Curie – Weiss equation, providing parameters of C = 9.06 cm^3 K mol^{-1} and θ = -5.34 K. In order to quantitatively evaluate magnetic interactions of polymer **3** for similar binuclear Mn^{2+} complexes, the following eq is induced from Hamiltonian $\hat{H} = -2J\hat{S}_1 \cdot \hat{S}_2$ [26]:

$$\chi_M = \frac{2Ng^2\mu_B^2}{KT}\left(\frac{\begin{array}{c}\exp(2J/KT) + 5\exp(6J/KT) + 14\exp(12J/KT) + \\ 30\exp(20J/KT) + 55\exp(30J/KT)\end{array}}{\begin{array}{c}1 + 3\exp(2J/KT) + 5\exp(6J/KT) + 7\exp(12J/KT) \\ +9\exp(20J/KT) + 11\exp(30J/KT)\end{array}}\right)$$

The fits lead to the following parameters for polymer **3**: J = -1.67 cm^{-1}, g = 2.01 and $R = 8.98\times10^{-4}$. ($R = \Sigma[(\chi_M)_{obs} - (\chi_M)_{calac}]^2/\Sigma[(\chi_M)_{obs}]^2$). The best fit is shown in figure 3c as a solid line.

In these complexes, the dominant pathways for magnetic exchange are carboxy group and double diazole-bridges. Previous magneto-structural considerations have identified that a larger symmetry of bridge affords a more effective overlap between the metal magnetic orbitals.[27] From the structure of these complexes, the bridges lead to relative less effective overlap between the orbitals. So the magnetic exchange intensities of the three complexes are weak.

Conclusions

In summary, hexanuclear-based **1** and octanuclear metallamacrocycle-based isostructure framework **2** and **3** have been obtained and characterised. In **1**, hexanuclear units are further connected by pbt^{2-} and $C_2O_4^{2-}$ resulting in the formation of two-dimensional layer. Further, the adjacent 2D layers in an offset way are arranged into three-dimensional supermolecular network by strong hydrogen-bonding interactions and π···π interactions. Octanuclear metallamacrocycles are linked by pbt^{2-} to construct the 3D isostructure **2** and **3**. In addition, left- and right-handed helical chains present alternately along the crystallographic c axis in the framework of **2** and **3**. Magnetic susceptibility measurements review that all of the complexes display antiferromagnetic couplings.

Acknowledgment.

This work was supported by the Henan Polytechnic University Foundation for Doctor Teachers (61307-002 and 72103-001-103) and the National Natural Science Foundation of China (Nos. 20971110 and 91022013).

References

1. a) Y. Y. Zhang, X. Y. Shen, L. H. Weng, and G. X. Jin, *J. Am. Chem. Soc.*, 2014, **136**, 15521. b) E. C. Yang, Y. Y. Zhang, Z. Y.i Liu, and X. J. Zhao, *Inorg. Chem.*, 2014, **53**, 327. c) M. J. Wiester, P. A. Ulmann and C. A. Mirkin, *Angew. Chem. Int. Ed*. 2011, **50**, 114. d) J. W. Sharples, D. Colloison. *Coord. Chem. Rev*. 2014, **260**, 1. e) B.Breiner, J. K. Cleqq, J. R. Nitschke. *Chem. Sci*. 2011, **2**, 51. f) G. A. Timco, T. B. Faust, F. Tuna and R. E. P. Winpenny. *Chem. Soc. Rev.* 2011, **40**, 3067.
2. a) E. C. Yang, Y. Y. Zhang, Z. Y. Liu, X. J. Zhao. *Inorg. Chem.*, **2014**, *53*, 327. b) J. Jankolovits, J. W. Kampf, and V. L. Pecoraro, *Inorg. Chem.*, 2013, **52**, 5063. c) K. Z. Su, F. L. Jiang, J. J. Qian, J. Pan, J. D. Pang, X. Y. Wan, F. L. Hu and M. C. Hong, *RSC Adv.*, 2015, **5**, 33579. d) M. D. Pluth and K. N. Raymond. *Chem. Soc. Rev*. 2007, **36**, 161. e) M. Yoshizawa, J. K. Klosterman and M. Fujita. *Angew. Chem. Int. Ed*. 2009, **48**, 3418. f) M. Albrecht and R. Fröhlich. *Bull. Chem. Soc. Jpn*. 2007, **80**, 797.
3. a) S. T. Wang, Y. F. Bi and W. P. Liao, *CrystEngComm*., 2015, **17**, 2896. b) Z. L. Fang, X. Y. Wu, R. M. Yu and C. Z. Lu, *CrystEngComm*., 2014, **16**, 8769. 8. M. D. Ward. *Chem. Commun*. 2009, **30**, 4487. c) D. L. Long, R. Tsunashima and L. Cronin. *Angew. Chem. Int. Ed.* 2010, **49**, 1736. d) R. W. Saalfrank, A. Scheurer. *Top. Curr. Chem*. 2012, **319**, 125. e) G. Mezei, C. M. Zaleski, and V. L. Pecoraro. *Chem. Rev*. 2007, **107**, 4933.
4. L. Han, L. Qin, X. Z. Yan, L. P. Xu, J. L. Sun, L. Yu, H. B. Chen, and X. D. Zou, *Cryst. Growth & Des.*, 2013, **13**, 1807.

5. K. C. Xiong, F. L. Jiang, Y. L. Gai, Z. Z. He, D. Q. Yuan, L. Chen, K. Z. Su, and M. C. Hong, *Cryst. Growth & Des.*, 2012, **12**, 3335.
6. a) M. A. Galindo, D. Olea, M. A. Romero, J. Gómez, P.Castillo, M. J. Hannon, A. Rodger, F. Zamora and J. R. Navarro, Chem.-Eur. J., 2007, **13**, 5075. B) Y. F. Bi, S. T. Wang, M. Liu, S. C. Du and W. P. Liao, *Chem. Commun*., 2013, **49**, 6785. C) Y. F. Bi, S. T. Wang, M. Liu, S. C. Du and W. P. Liao, *Chem. Commun.*, 2013, **49**, 6785.
7. a) H. A. Burkill, N. Robertson, R. Vilar, A. J. P. White, and D. J. Williams, *Inorg. Chem.*, 2005, **44**, 3337. b) S. Chorazy, R. Podgajny, K. Nakabayashi, J. Stanek, M. Rams, B. Sieklucka and S. Ohkoshi, *Angew. Chem. Int. Ed*., 2015, **54**, 5093. c) L. Chatelain, J. P. S. Walsh, J. Pécaut, F. Tuna and M. Mazzanti, *Angew. Chem. Int. Ed*., 2014, **53**, 13434.
8. a) S. K. Langley, B. Moubaraki, C. Tomasi, M. Evangelisti, E. K. Brechin, and K. S. Murray, *Inorg. Chem.*, 2014, **53**, 13154. b) A. K. Jassal, S. Sharma, G. Hundal, and M. S. Hundal, *Cryst. Grow. & Des*., 2015, **15**, 79. c) W. J. Chu, B. L. Wu, M. S. Tang, Y. T. Fan and H. W. Hou, *CrystEngComm*., 2012, **14**, 4414. d) Z. Q. Xu, Q. Wang, H. J. Li, W. Meng, Y. Han, H. W. Hou and Y. T. Fan , *Chem. Commun.*, 2012, **48**, 5736. e) H. Ida, T. Shiga, G. N. Newton and H. Oshio, *Inorg. Chem. Front.*, 2015, **2**, 538.
9. F. P. Xiao, J. Hao, J. Zhang, C. L. Lv, P. C. Yin, L. S, Wang and Y. G. Wei, *J. Am. Chem. Soc.*, 2010, **132**, 5956.
10. J. Y. Hu, J. A. Zhao, Q. Q. Guo, H. W. Hou and Y. T. Fan, *Inorg. Chem.*, 2010, **49**, 3679.
11. a) L. Hsiu-Mei and C. Tsung-Yuan, *Cryst. Growth & Des.*, **2009**, 9, 2988. b). S. K. Langley, B. Moubaraki, K. J. Berry and K. S. Murray. *Dalton Trans*., 2010, **39**, 4848. c). A. A. Athanasopoulou, M. Pilkington, C. P. Raptopoulou, A. Escuer and T. C. Stamatatos. *Chem. Commun*., 2014, **50**, 14942. d). C. Plenk, T. Weyhermüller and E. Rentschler. *Chem. Commun*., 2014, **50**, 3871.
12. a) I. Fernández, R. Ruiz, J. Faus, M. Julve, F. Lloret, J. Cano, X. Ottenwaelder, Y. Journaux and M. C. Muñoz, *Angew. Chem. Int. Ed*., 2001, **40**, 3039. b). T. Nakajima, K. Seto, F. Horikawa, I. Shimizu, A. Scheurer, B. Kure, T. Kajiwara, T. Tanase, and M. Mikuriya. *Inorg. Chem*. 2012, **51**, 12503. c). A. Baniodeh, Y. Liang, C. E. Anson, N. Magnani, A. K. Powell, A. Unterreiner, S. Seyfferle, M. Slota, M. Dressel, L. Bogani. *Adv. Funct. Mater*. 2014, **24**, 6280.
13. C. M. Che, B. H. Xia, J. S. Huang, C. K. Chan, Z. Y. Zhou and K. K. Cheung, *Chem. -Eur. J.*, 2001, **13**, 3998.
14. C. Kaes, M. W. Hosseini, C. E. F. Rickard, B. W. Skelton and A. H. White, *Angew. Chem. Int. Ed*., 1998, **37**, 920.
15. Y. Kikukawa, Y. Kuroda, K. Yamaguchi and N. Mizuno, *Angew. Chem. Int. Ed*., 2012, **51**, 2434.
16. a) Z. M. Zhang, Y. G. Li, S. Yao, E. B. Wang, Y. H. Wang and R. Clérac, *Angew. Chem. Int. Ed*., 2009, **48**, 1581. B) L. R. Piquer and E. C. Sañudo, *Dalton Trans.*, 2015, **44**, 8771. c) J. Liu, Y. C. Chen, Z. X. Jiang, J. L. Liu, J. H. Jia, L. F. Wang, Q. W. Li and M. L. Tong, *Dalton Trans.*, 2015, **44**, 8150. d) Z. Y. Liu, H. Y. Zhang, E. C. Yang, Z. Y. Liu and X. J. Zhao , *Dalton Trans.*, 2015, **44**, 5280.
17. a) X. L. Wang, C. H. Gong, J. W. Zhang, G. C. Liu, X. M. Kan and N. Xu, *CrystEngComm.*, 2015, **17**, 4179. b) Y. Y. Wang, Q. Jin, S. X. Liu, C. Guo, Y. Y. Liu, B. Ding, X. X. Wu, Y. Li and Z. Z. Zhu, ***RSC Adv.***, 2015, **5**, 35238.
18. a) S. T. Wang, Y. F. Bi and W. P. Liao , *CrystEngComm*., 2015, **17**, 2896. b) R. P. John, K. Lee, B. J. Kim, B. J. Suh, H. Rhee, and M. S. Lah, *Inorg. Chem.*, 2005, **44**, 7109. c) H. A. Burkill, N. Robertson, R. Vilar, A. J. P. White, and D. J. Williams. *Inorg. Chem.*, 2005, **44**, 3337.
19. a) F. Meier, D. Loss, *Phys. Rev. B*., 2001, **64**, 224411; b) F. Meier, D. Loss, *Phys. Rev. Lett.*, 2001, **86**, 5373; c) O. Waldmann, T. C. Stamatatos, G. Christou, H. U. Güdel, I. Sheikin, H. Mutka, *Phys. Rev. Lett.*, 2009, **102**, 157202.
20. a) W. Q. Lin, J. D. Leng, M. L. Tong, *Chem. Commun*., 2012, **48**, 4477; b) Y. B; Dong, Q. Zhang, L. L. Liu, J. P. Ma, B. Tang, R. Q. Huang, *J. Am. Chem. Soc.*, 2007, **129**, 1514; c) C. Y. Su, A. M. Goforth, M. D. Smith, P. J. Pellechia, Loye, H. C. *J. Am. Chem. Soc.*, 2004, **126**, 3576; d) W. C. Song, Q. H. Pan, P. C. Song, Q. Zhao, Y. F. Zeng, T. L. Hu, X. H. Bu, *Chem. Commun*., 2010, **46**, 4890.
21. a) L. Yi, B. Ding, B. Zhao, P. Cheng, D. Z. Liao, S. P. Yan, Z. H. Jiang, *Inorg. Chem*., 2004, **43**, 33; c) S. Ferrer, E. Aznar, F. Lloret, A. Castiñeiras, M. Liu-González, J. Borrás, *Inorg. Chem*., 2007, **46**, 372.
22. a) W. Ouellette, A. V. Prosvirin, J. Valeich, K. R. Dunbar, J. Zubieta, *Inorg. Chem*., 2007, **46**, 9067; b) A. Noble, J. Olguin, R. Clerac, S. Brooker, *Inorg. Chem*., 2010, **49**, 4560; c) O. A. Bondar, L. V. Lukashuk, A. B. Lysenko, H. Krautscheid, E. B. Rusanov, A. N. Chernega, K. V. Domasevitch, *CrystEngComm*., 2008, **10**, 1216.
23. a) J. Hernández-Gil, S. Ferrer, A. Castiñeiras, F. Lloret, *Inorg. Chem*., 2012, **51**, 9809; b) P. M. Slangen, P. J. Koningsbruggen, K. Goubitz, J. G. Haasnoot, J. Reedijk, *Inorg. Chem*. 1994, **33**, 1121; c) X. Bao, J. L. Liu, J. D. Leng, Z. Lin,; M. L. Tong, M. Nihei, H. Oshio, *Chem. Eur. J.,* 2010, **16**, 7973.
24. G. M. Sheldrick, *Acta Crystallogr., Sect. A: Found. Crystallogr.*, 2008, **A64**, 112.
25. Q. P Li, C. B. Tian, H. B. Zhang, J. J. Qian and S. W. Du. *CrystEngComm*., 2014, **16**, 9208.
26. (a) R. L. Carlin, *Magnetochemistry, Springer, Berlin*, 1986. (b) L.Y. Xin, G. Z. Liu, X. L. Li, and L. Y. Wang. *Cryst. Growth Des.*, 2012, **12**, 147.
27. (a) W. Ouellette, A. V. Prosvirin, J. Valeich, K. R. Dunbar, J. Zubieta, *Inorg. Chem*., 2007, **46**, 9067; (b) A. Noble, J. Olguń, R. Clerac, S. Brooker, *Inorg. Chem.*, 2010, **49**, 4560.

For Table of Contents Use Only

Construction of Fe6, Fe8 and Mn8 Metallamacrocyclic Complexes and Magnetic Properties

Huijun Li,[a] Yuan Wang,[a] Hongxin Cai,[a] Zhouqing Xu *[a], Lei Jia*[a] and Hongwei Hou*[b]

Hexanuclear-based **1** and octanuclear metallamacrocycle-based three-dimensional isostructural framework **2** and **3** have been obtained and characterised. Magnetic susceptibility measurements show that the three complexes display antiferromagnetic couplings.